ACS ES&T Water

pubs.acs.org/estwater

Article

Directional Oxidation of Amine-Containing Phenolic Pharmaceuticals by Aqueous Dissolved Oxygen under Dark Conditions Catalyzed by Nitrogen-Doped Multiwall Carbon Nanotubes

Langsha Yi, Chenhui Wei, Wanchao Yu, Heyun Fu, Xiaolei Qu, Pedro J. J. Alvarez, and Dongqiang Zhu*

Cite This: *ACS EST Water* 2021, 1, 79–88

Read Online

ACCESS | Metrics & More | Article Recommendations | Supporting Information

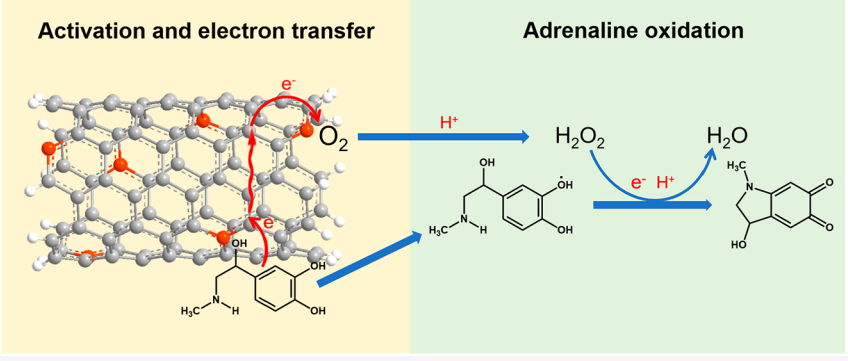

ABSTRACT: As a widely used class of pharmaceuticals, amine-containing phenolic compounds are commonly found in water systems, which has raised growing concern about their potential health impact and requires effective treatment technologies that minimize the need for chemical addition. Here, we report efficient oxidation of three representative amine-containing phenolic pharmaceuticals (e.g., adrenaline, dopamine, and paracetamol) in the presence of nitrogen-doped multiwall carbon nanotubes (150 mg/L), which were transformed to adrenochrome, dopaminechrome, and benzoquinone, respectively, as the sole products at 25 °C in the dark without adding oxidants. The yield was 100% for adrenochrome in 30 min, 95% for dopaminechrome in 120 min, and 62% for benzoquinone in 120 h. In contrast, no oxidation occurred in the presence of nondoped carbon nanotubes or graphene oxides, or pure graphite. Inhibition of reactive oxygen species (ROS) combined with electron paramagnetic resonance analysis and continuous flow chemiluminescence measurement showed that self-catalyzed production of hydrogen peroxide (H_2O_2, maximum of 0.13 mM with 0.18 mM adrenaline) was the driving mechanism for the directional catalytic oxidation. The importance of adsorption of adrenaline to the oxidation reaction was verified by the linear relationship observed between the reciprocal of the initial oxidation rate and the reciprocal of the initial adrenaline concentration complying with the Langmuir−Hinsheiwood model as well as the effect of pH-dependent adsorption on the oxidation kinetics. These results provide new insight into nano-enabled self-catalyzed production of ROS, which might be exploited for the treatment of similarly structured chemicals.

KEYWORDS: *phenolic compounds, nitrogen-doped multiwall carbon nanotubes, reactive oxygen species, electron paramagnetic resonance, continuous flow chemiluminescence*

INTRODUCTION

In recent years, human pharmaceutical compounds including amine-containing phenols (ACPs) have been increasingly detected in sewage water,[1,2] surface water,[3,4] and even drinking water.[5,6] ACPs make up a class of commonly used pharmaceuticals and are produced in large quantities for the treatment of many diseases. For example, paracetamol is currently the most widely used antipyretic and analgesic drug, and adrenaline and dopamine are often used to treat cardiac resuscitation, hypertension, shock, and asthma in clinical emergency.[7,8] Most ACPs used in medical treatment are excreted via feces and urine as unmodified parent compounds, with only small fractions being metabolized. For example, a previous study reported that 58−68% of paracetamol taken by human is excreted from the body.[7] As a result, large amounts

Received: June 2, 2020
Revised: July 2, 2020
Accepted: July 20, 2020
Published: August 11, 2020

of ACPs are discharged into municipal wastewater and consequently into surface water owing to their low biodegradability in conventional treatment systems.[9,10] Concentrations of paracetamol as high as tens of micrograms per liter are being detected in sewage water and even fresh water.[11,12] Residues of ACPs present in waters have raised growing public health concerns. Previous studies showed that paracetamol, adrenaline, and dopamine may cause hepatotoxicity, neurotoxicity, myocardial toxicity, and possible carcinogenicity based on animal toxicity tests.[13−16]

Advanced oxidation processes (AOPs) are effective for removing a variety of recalcitrant organic contaminants at low concentrations during water and wastewater treatment. Reactive oxygen species (ROS), including hydroxyl radical (•OH), hydrogen peroxide (H_2O_2), and ozone (O_3), and other oxidative free radicals such as sulfate radicals ($SO_4^{\bullet-}$) generated through activation of oxidants by transition metals (iron), photoexcitation, and/or electrochemistry are used by AOPs to degrade organic contaminants.[17−20] Despite the high treatment efficiency, the use of AOPs is challenged not only by extensive use of chemicals and high energy requirements but also by secondary contamination stemming from uncontrollable reaction pathways and side product formation, and in some cases metal leaching.[21,22]

Engineered carbon nanomaterials (including carbon nanotubes, fullerenes, and graphenes) have shown great potential for advancing AOPs in water and wastewater treatment.[21] One unique feature of carbon nanomaterials is that their surface chemistry can be tuned to achieve specific and enhanced adsorption and catalytic properties.[23,24] Doping heteroatoms (such as N and B) into the graphitic lattice of carbon nanomaterials is a powerful tuning methodology for inducing new electronic states and increasing the rate of electron transfer toward superior catalytic activity and selectivity.[25,26] For instance, nitrogen-doped carbon nanomaterials (as inexpensive nonmetal catalysts) exhibit high activity and durability for catalytic oxidation.[26,27] The carbon atoms with Lewis basicity next to pyridinic nitrogen atoms serve as the active site to facilitate the weakening of the O−O bond of the adsorbed oxygen molecule and in turn its acceptance of electrons during the redox reaction.[26] Similarly, nitrogen-doped carbon nanomaterials can activate other oxidants (including peroxymonosulfate and H_2O_2) and generate free radicals ($SO_4^{\bullet-}$ and •OH) for oxidation of organic contaminants, which can be classified as a nano-enabled AOP technique for water treatment.[28−30] These observations suggest that nitrogen-doped carbon nanomaterials may catalyze the oxidation of ACPs by activating oxidants as ROS precursors.

The main objective of this study was to assess whether nitrogen-doped carbon nanotubes can catalyze the light-independent self-catalyzed oxidation of selected ACPs by dissolved oxygen under mild conditions without adding any chemical oxidizing agent. Additional carbonaceous materials including nondoped carbon nanotubes and graphene oxides and pure graphite were included as benchmarks for comparison. A series of experiments were systematically designed to illustrate the possible underlying catalytic mechanisms, including specific ROS scavenging tests and spectroscopic measurements. Therefore, this paper informs a novel, precise oxidation process that could minimize energy and chemical requirements for initiating the degradation of recalcitrant organic compounds.

MATERIALS AND METHODS

Chemicals and Materials. The three tested compounds are adrenaline (99.8%, Targetmol, Shanghai, China), dopamine (99%, Sigma-Aldrich, St. Louis, MO), and paracetamol (98%, Tokyo Chemical Industry). Their molecular structures and stepwise acid dissociation constants (pK_{as}) are listed in Figure S1. Isopropyl alcohol (IPA, >99%), superoxide dismutase (SOD, 2500−7000 units/mg, from pig blood), catalase (CAT, 5000 units/mg, from bovine liver), *o*-chlorophenol (CP, >98%), hydrogen peroxide (H_2O_2, 30%), 5,5-dimethyl-1-pyrroline *N*-oxide (DMPO, 97%), tetramethylpiperidine (TEMP, 98%), 5-amino-2,3-dihydro-1,4-phthalazinedione (Luminol, 97%), 2,4,6-trimethylphenol (TMP, 97%), and benzoquinone (>98%) were purchased from Sigma-Aldrich. Deuteroxide (D_2O, 99.8 atom % D) was purchased from Tokyo Chemical Industry. 3-Hydroxy-1-methyl-5,6-indolinedione (Adrenochrome, 99%) was purchased from Toronto Research Chemicals (Toronto, ON). Analytical grade sodium dihydrogen phosphate (NaH_2PO_4), disodium hydrogen phosphate (Na_2HPO_4), potassium dihydrogen phosphate (KH_2PO_4), phosphoric acid (H_3PO_4), sodium hydroxide (NaOH), dimethyl sulfoxide (DMSO), and potassium ferricyanide [$K_3Fe(CN)_6$] were purchased from Sinopharm Chemical Reagent Co., Ltd. (Shanghai, China). Methanol of LC-MS grade was obtained from Fisher Scientific. Ultrapure deionized (DI) water (18.2 MΩ cm) prepared by an ELGA Labwater system (PURELAB Ultra, ELGA LabWater Global Operations) was used during all experiments.

Nitrogen-doped multiwall carbon nanotubes (N-MCNT) were synthesized by chemical vapor deposition of pyridine on Fe−Co catalysts supported on Al_2O_3 powder using a method similar to that described in the literature.[31] The synthesized N-MCNT sample was treated successively with 6 M NaOH at 110 °C to remove Al_2O_3 and 6 M HCl at 110 °C to remove Fe−Co catalyst, followed by a DI water rinse and drying. Multiwall carbon nanotubes (MCNT) were purchased from Macklin Co. (Shanghai, China). According to the information provided by the manufacturer, MCNT were also synthesized by the chemical vapor deposition method and contained carbon nanotubes with inner diameters ranging from 5 to 15 nm, outer diameters of >50 nm, lengths from 10 to 20 nm, and <10% impurities. The MCNT sample was treated by being heated (350 °C for 30 min) and then mixed with a 70% (w/v) sodium hypochlorite (NaClO) aqueous solution and a 2.5% nitric acid (HNO_3) solution to remove amorphous carbon and metal catalyst.[32] Pure graphite (>99% carbon, J&K Chemical) and graphene oxides (GO) (>99%, XFNANO Materials Tech, Jiangsu, China) were selected as additional benchmarks for performance comparison.

Characterization of Carbonaceous Materials. X-ray photoelectron spectroscopy (XPS, Shimadzu AXIS Supra, Kratos) was applied to quantify the surface elemental compositions of the carbonaceous materials. The specific surface area (SSA) was measured using an accelerated surface area and porosimetry system (ASAP2020, Micromeritics) by N_2 adsorption and desorption isotherms. To assess surface hydrophilicity, the contact angle of a water droplet of MCNT or N-MCNT was measured by a contact angle goniometer (Powereach, JC2000D). The morphological features and elemental mapping images of N-MCNT were achieved using field-emission high-resolution transmission electron micros-

https://dx.doi.org/10.1021/acsestwater.0c00003
ACS EST Water 2021, 1, 79−88

copy (FE-HRTEM, JEM-2100F, JEOL) coupled with energy-dispersive X-ray spectroscopy (EDS).

Catalytic Oxidation of Organic Compounds. The oxidation reaction kinetics of adrenaline, dopamine, and paracetamol was measured by using a 200 mL glass batch reactor at 25 °C. Briefly, 30 mg of carbonaceous material was sonicated in 200 mL of an aqueous solution containing 5 mM phosphate buffer (pH 6) for 20 min to disperse solid particles homogeneously and then magnetically stirred for 12 h, followed by addition of the target compound. The initial concentration was 0.18 mM for adrenaline and dopamine and 0.05 mM for paracetamol. The reactor was covered with aluminum foil during the reaction to prevent any light irradiation. An aliquot of 0.5 mL was withdrawn at the desired time intervals and mixed with 2 mL of methanol in a 4 mL amber glass vial equipped with polytetrafluoroethylene-lined screw cap. The mixture was then vortexed and sonicated to disperse the carbonaceous material for extraction of the target compound and possible reaction product(s) and filtered through a 0.22 μm filter for analysis. The recovery of the three ACPs was nearly 100% if no oxidation occurred after removal of dissolved oxygen by nitrogen (99.999%) purging. The adsorption ratio of the three ACPs to N-MCNT (measured in the absence of oxygen) was ~15%. To evaluate the role of self-catalyzed reactive species, various quenching agents, including CAT for H_2O_2,[33] SOD for superoxide ions ($O_2^{\bullet-}$),[34] IPA for •OH,[35] TMP for triplet-state organics,[36] and CP for a hydrated electron (e_{aq}^-),[37] were used for the inhibition of oxidation of the three target compounds in the presence of N-MCNT. To test the role of dissolved oxygen, the suspension of N-MCNT was purged with N_2 for at least 1 h to remove dissolved oxygen prior to spiking of each compound, and the operation was performed in a glovebox filled with N_2. The catalytic oxidation of the three compounds in the presence of N-MCNT was also measured in mixtures of D_2O and H_2O [90:10 (v/v)]. Compared with H_2O, D_2O significantly increases the lifetime of singlet oxygen ($^1O_2$) due to the kinetic solvent isotope effect.[38] Moreover, the catalytic oxidation of the three compounds was conducted using neat DMSO (a proton-free solvent). To assess the possible involvement of H_2O_2, the oxidation of adrenaline by extra H_2O_2 added at varying concentrations (1−100 mM) was measured in the presence and absence of N-MCNT. In addition, the potential effects of initial compound concentrations (0.04−0.18 mM) and pH (3−7, buffered with 5 mM phosphate buffer) on the catalytic oxidation of adrenaline by N-MCNT were examined. All oxidation reaction experiments were performed in duplicate.

A high-performance liquid chromatography (HPLC, Agilent 1200) equipped with a Zorbax SB-C18 column (Agilent) was applied to analyze the concentrations of adrenaline, dopamine, and paracetamol. The isocratic elution and detection were performed under the following conditions: 98% 0.02 M KH_2PO_4 and 2% methanol (v/v) and fluorescence excitation and emission at 280 and 316 nm, respectively, for adrenaline; 98% 0.02 M KH_2PO_4 and 2% methanol (v/v) and ultraviolet (UV) absorption at 254 nm for dopamine; 80% water and 20% methanol (v/v) and UV absorption at 254 nm for paracetamol. Oxidation reaction products including adrenochrome from adrenaline and dopaminechrome from dopamine were identified by Fourier transform ion cyclotron resonance mass spectrometry (FT-ICRMS, Solarix XR, Bruker), and benzoquinone from paracetamol was identified by high-performance liquid chromatography combined with photodiode-array detection and time-of-flight mass spectrometry (HPLC-DAD-TOF-MS, Triple TOF5600$^+$, AB Sciex). More analytical details are given in Text S1 of the Supporting Information.

Measurement of Reactive Oxygen Species. The possible formation of •OH, $O_2^{\bullet-}$, and $^1O_2$ during the oxidation reaction of adrenaline was measured using a Bruker EMX-10/12 electron paramagnetic resonance (EPR) spectrometer (Bruker) with a resonance frequency of 9.8 GHz, a modulation amplitude of 1.0 G, a modulation frequency of 100 kHz, a microwave power of 20 mW, a sweep width of 200 G, a time constant of 40.96 ms, a receiver gain of 30 db, and a sweep time of 20 s. DMPO was used as a spin trapping agent for $O_2^{\bullet-}$ and •OH, and TEMP for $^1O_2$ in EPR analysis.[39,40] The two carbon nanotubes before and after the oxidation reaction of adrenaline in the presence of dissolved oxygen were also measured by EPR using the same parameter settings as described above but without any spin-trapping agent. An oxygen microsensor (Microx 4 PreSens, Precision Sensing GmbH) was used to measure dissolved oxygen. The production of H_2O_2 and $O_2^{\bullet-}$ during the oxidation of adrenaline was quantified using a continuous flow chemiluminescence (CFCL) system.[41] Briefly, the reaction suspension containing adrenaline and N-MCNT prepared using the same experimental setup and conditions as described above was continuously pumped with a peristaltic pump and mixed with the CL probe (Luminol) pumped from another peristaltic pump in a 5 mL spiral detection cell. The CL signal was produced by a redox chemical reaction between Luminol and ROS. For $O_2^{\bullet-}$ measurement, Luminol alone was used; for H_2O_2 measurement, in addition to Luminol, $K_3Fe(CN)_6$ (a signal enhancer) was also pumped into the detection cell by a separate peristaltic pump. The CL intensity was then measured by a photomultiplier tube (PMT) and converted to the concentration of H_2O_2 or $O_2^{\bullet-}$. The schematic diagram of the CFCL system and experimental details are presented in Figure S2.

RESULTS AND DISCUSSION

Characterization of N-MCNT and MCNT. The specific surface areas and surface elemental compositions of the tested carbonaceous materials are listed in Table 1. N-MCNT, MCNT, and graphene oxides had relatively large specific surface areas ranging from 121.8 m^2/g (MCNT) to 201.3 m^2/g (graphene oxides), while pure graphite had the smallest (5.1 m^2/g). The surfaces of all of the carbonaceous materials were dominated by carbon (71.9−99.3%), and their surface oxygen

Table 1. Surface Elemental Compositions (dry weight-based) and Specific Surface Areas (SSA) of Different Carbonaceous Materials

	surface elemental composition[a] (%)			
sample	C	O	N	SSA[b] (m^2/g)
MCNT	96.19	3.81	BDL[c]	121.8
N-MCNT	94.29	2.52	3.19	162.2
graphite	99.30	0.7	BDL[c]	5.1
graphene oxides	71.91	28.09	BDL[c]	201.3

[a]Measured by X-ray photoelectron spectroscopy. [b]Measured by N_2 adsorption using the Brunauer−Emmett−Teller method. [c]Below the detection level.

https://dx.doi.org/10.1021/acsestwater.0c00003
ACS EST Water 2021, 1, 79−88

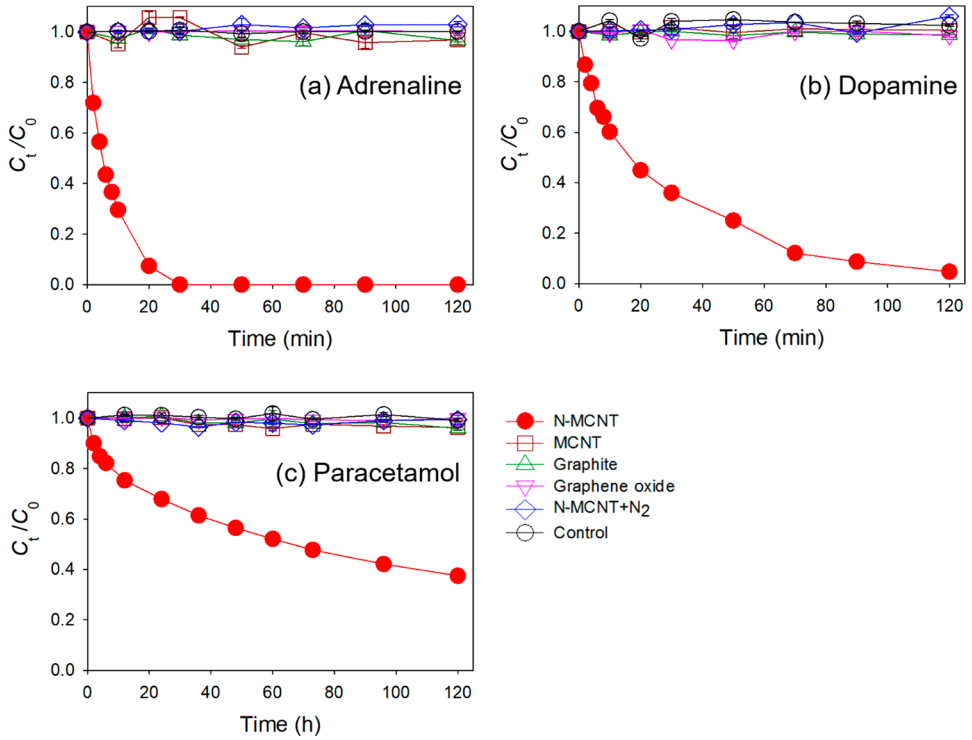

Figure 1. Degradation of ACPs plotted as the ratio of the concentration at a given time (C_t) to the initial concentration (C_0) vs time without (Control) and with different carbonaceous materials (150 mg/L) at pH 6 with phosphate buffer. (a) Adrenaline (initially at 0.18 mM). (b) Dopamine (initially at 0.18 mM). (c) Paracetamol (initially at 0.05 mM). Error bars represent standard variations calculated from duplicate samples. Lines are for visual clarity only.

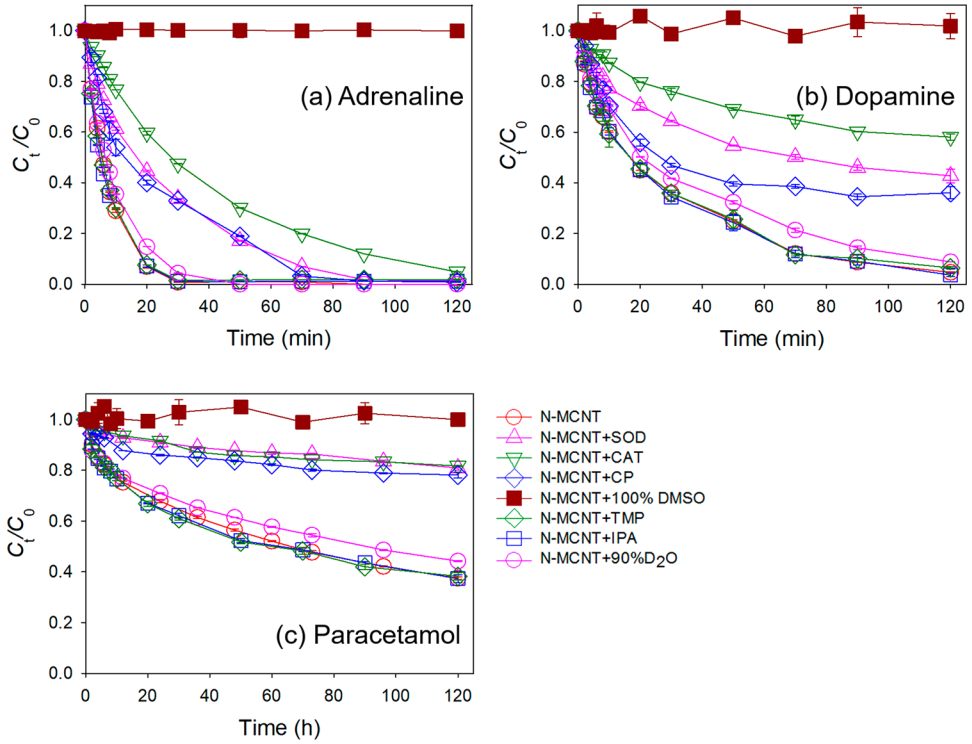

Figure 2. Degradation of ACPs plotted as the ratio of the concentration at a given time (C_t) to the initial concentration (C_0) vs time in the presence of N-MCNT (150 mg/L) under different conditions at pH 6 with phosphate buffer (except for DMSO). (a) Adrenaline (initially at 0.18 mM). (b) Dopamine (initially at 0.18 mM). (c) Paracetamol (initially at 0.05 mM). Error bars represent standard variations calculated from duplicate samples. Lines are for visual clarity only.

compositions varied from 0.7% (graphite) to 28.1% (graphene oxides). The two carbon nanotubes had very similar surface elemental compositions except that N-MCNT had 3.2% nitrogen. Deconvolution of the nitrogen envelope in the XPS

https://dx.doi.org/10.1021/acsestwater.0c00003
ACS EST Water 2021, 1, 79−88

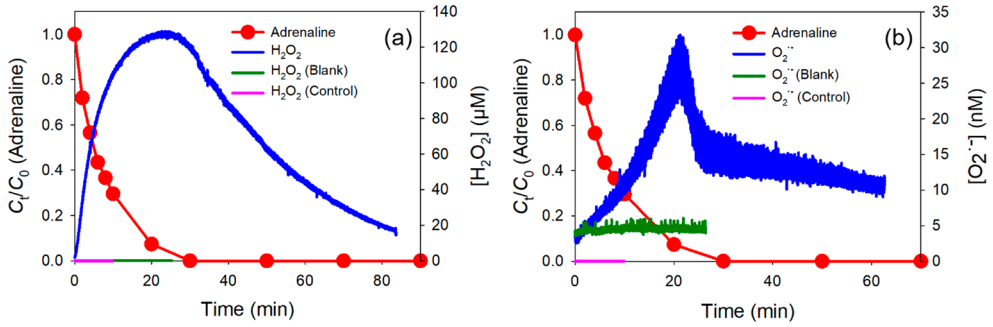

Figure 3. Production of H_2O_2 and $O_2^{\bullet-}$ plotted as the time-dependent change in concentration, (a) $[H_2O_2]$ and (b) $[O_2^{\bullet-}]$, along with degradation of adrenaline (initially at 0.18 mM) plotted as the ratio of the concentration at a given time (C_t) to the initial concentration (C_0) vs time without (Control) and with N-MCNT (150 mg/L) at pH 6 with phosphate buffer. Blank refers to samples containing N-MCNT but no adrenaline. Lines shown for adrenaline are for visual clarity only.

spectra of N-MCNT demonstrated the presence of graphitic N (53.1%), pyridinic N (28.3%), and nitrogen oxides (18.6%). The elemental mapping measured by HRTEM-EDS showed that the nitrogen atoms were evenly distributed on the surface of N-MCNT (Figure S3). The water contact angle of N-MCNT (41.8°) was considerably smaller than that of MCNT (66.8°) (Figure S4), indicating the much lower surface hydrophobicity of N-MCNT, which can be ascribed to the polar nitrogen-containing functional groups.

Kinetics of N-MCNT-Catalyzed Oxidation of ACPs. Figure 1a–c displays the loss of the three tested ACPs, adrenaline (initially at 0.18 mM), dopamine (initially at 0.18 mM), and paracetamol (initially at 0.05 mM), as a function of time in the presence of different carbonaceous materials. Significant degradation of the three ACPs was observed with N-MCNT. The degradation kinetics decreased in the following order: adrenaline > dopamine > paracetamol. The removal efficiency was 100% at 30 min for adrenaline, 95% at 120 min for dopamine, and 63% at 120 h for paracetamol. The degradation kinetics was best described by the pseudo-first-order model (R^2 > 0.96) for adrenaline and dopamine and by the pseudo-second-order model (R^2 = 0.99) for paracetamol (fitting parameters summarized in Table S1). In contrast, no compound degradation occurred in the presence of MCNT, graphene oxides, or pure graphite. Similarly, no compound degradation was observed in the presence of N-MCNT following removal of dissolved oxygen by nitrogen purging, suggesting that the degradation of the three ACPs was induced by ROS generated from dissolved oxygen. With the aid of high-resolution mass spectroscopy analysis, adrenochrome, dopaminechrome, and benzoquinone were identified as the sole oxidation products of adrenaline, dopamine, and paracetamol, respectively (Text S1 and Figures S5–S7). This indicates that unlike other AOPs that generally result in random and uncontrollable oxidation pathways with numerous byproducts (such as low-molecular weight ketones and organic acids),[42,43] these oxidation processes mediated by N-MCNT were precise and unidirectional. For all three ACPs, the phenolic group(s) was oxidized to a quinone group(s). The oxidation pathways of the three chemicals are presented in Figures S8 and S9. The mass balance (sum of parent compound and product) measured for the oxidation of adrenaline was 100%.

With regard to the accumulation of byproducts, it is noteworthy that complete mineralization is seldom achieved by AOPs,[43,44] and oxidative transformations may serve as a pretreatment step to detoxify recalcitrant contaminants and enable subsequent biodegradation.[45,46] However, further work would be needed to assess the ecotoxicity and biodegradability implications of the observed transformations in this work, which focuses on advancing our mechanistic understanding of a directed (possibly incidental) oxidation process rather than technology development.

Identification of Reactive Species Involved in the Oxidation of ACPs. To probe the self-catalyzed reactive species involved in the reaction, we examined the effects of inhibition on the oxidation of the three ACPs by a variety of scavengers, including CAT for H_2O_2, SOD for $O_2^{\bullet-}$, CP for e_{aq}^-, IPA for •OH, and TMP for triplet-state organics (Figure 2). The presence of CAT (40 mg/L), SOD (20 mg/L), and CP (50 mM) caused pronounced suppression of the oxidation of the three ACPs (the compound loss ratio at the end of the reaction decreased by 33–81%), suggesting that H_2O_2, $O_2^{\bullet-}$, and e_{aq}^- were involved in the oxidation or production of ROS responsible for oxidation. Among the tested scavengers, CAT exhibited the strongest suppression effect. The oxidation efficiency (ratio of compound loss) at the end of the reaction was remarkably decreased by 47%, 57%, and 81% for adrenaline, dopamine, and paracetamol, respectively. Thus, H_2O_2 likely played a dominant role in the oxidation of ACPs. In contrast, there was no obvious suppression by IPA or TMP, indicating that •OH and triplet-state organics were not involved in the reaction. After the reaction solvent had been changed from neat H_2O to a mixture of H_2O and D_2O [1:9 (v/v)], the oxidation of the three ACPs was almost unaffected. As D_2O can significantly increase the lifetime of $^1O_2$,[38] the results ruled out the possibility that $^1O_2$ was the key species responsible for the oxidation of ACPs. Consistent with the observed scavenger inhibition effects, EPR analysis verified the formation of $O_2^{\bullet-}$ during the oxidation of adrenaline in the presence of N-MCNT (Figure S10), whereas •OH and $^1O_2$ were not detected. Moreover, the oxidation of the three ACPs was completely terminated when switching the phosphate buffer solution to neat DMSO. DMSO is an effective scavenger of •OH but not of H_2O_2.[47,48] Thus, reaction termination by DMSO cannot be ascribed to quenching of ROS. As DMSO is a proton-free solvent, it can thus be determined that proton involvement is a prerequisite for the oxidation of ACPs.

Figure 3 displays H_2O_2 and $O_2^{\bullet-}$ concentrations as a function of time determined by CFCL analysis in the presence of N-MCNT, along with the oxidation decay of adrenaline. For both H_2O_2 and $O_2^{\bullet-}$, their concentrations increased during the reaction and peaked at the time when adrenaline was about to

https://dx.doi.org/10.1021/acsestwater.0c00003
ACS EST Water 2021, 1, 79–88

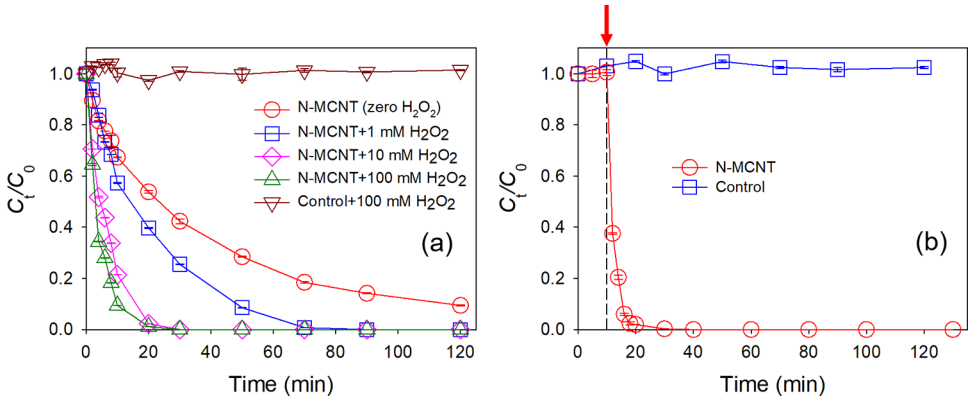

Figure 4. Degradation of adrenaline (initially at 0.18 mM) plotted as the ratio of the concentration at a given time (C_t) to the initial concentration (C_0) vs time without (Control) and with N-MCNT (50 mg/L) at pH 6 with phosphate buffer. (a) With extra H_2O_2 added at varying concentrations. (b) With removal of dissolved oxygen by N_2 purging prior to the reaction initiated by the addition of H_2O_2 (10 mM) at 10 min (denoted with an arrow). Error bars represent standard variations calculated from duplicate samples. Lines are for visual clarity only.

be completely removed. In the presence of only N-MCNT or adrenaline (but not both together), the production of H_2O_2 and $O_2^{\bullet-}$ was negligible. This indicates that these two ROS were generated by sensitization of adrenaline at the surface of N-MCNT. Moreover, the maximum concentration (0.13 mM) of H_2O_2 produced was relatively high and even comparable with the initial concentration (0.18 mM) of adrenaline and was >4000-fold higher than the maximum concentration (3.2×10^{-5} mM) of $O_2^{\bullet-}$. This corroborates the predominance of H_2O_2 in adrenaline oxidation. The important role played by H_2O_2 was further illustrated by the enhanced oxidation of adrenaline by extra H_2O_2 (1, 10, or 100 mM) added to the reaction system (Figure 4a). With an increasing concentration of added H_2O_2, the oxidation efficiency of adrenaline gradually increased and reached the highest point (91% at 10 min) at the highest added concentration (100 mM) of H_2O_2. However, in the absence of N-MCNT, no oxidation of adrenaline was shown even if extra H_2O_2 was added (Figure 4a). After removal of dissolved oxygen by nitrogen purging, no oxidation of adrenaline occurred even in the presence of N-MCNT. Furthermore, adrenaline degradation could be initiated by addition of H_2O_2 (10 mM) in the presence of N-MCNT, but not without N-MCNT (Figure 4b). These results demonstrate that H_2O_2 could oxidize adrenaline, but only when it was activated by N-MCNT.

Mechanisms for N-MCNT-Induced Oxidation of ACPs. Previous studies have reported that nitrogen-doped carbon nanomaterials can catalyze the reduction of adsorbed oxygen molecules by accepting conduction electrons to turn them into ROS (such as H_2O_2 and $O_2^{\bullet-}$), namely the oxygen reductive reaction (ORR), which is a key reaction for fuel cells and other renewable energy technologies.[24,27] In addition to the enhanced electronic conductivity, the catalysis activity of nitrogen-doped carbon nanomaterials is mainly attributed to the weakening of the O−O bond of oxygen molecules due to the strong chemosorptive interaction with the carbon atoms with Lewis basicity next to pyridinic N.[26] Consistently, the adsorption ratio of dissolved oxygen (initially at 8.32 mg/L in a pH 6 phosphate buffer solution) was much higher with N-MCNT (7 ± 2%, standard deviation calculated from three replicates) than with MCNT (0.7 ± 0.3%) given the same sorbent dose (2500 mg/L). However, in the absence of adrenaline, no ROS (H_2O_2 and $O_2^{\bullet-}$) was generated by N-MCNT (Figure 3).

We here propose the mechanisms for N-MCNT-induced oxidation of ACPs using adrenaline as an example. First, N-MCNT simultaneously activate the adsorbed oxygen molecules and adrenaline molecules at the activation sites. Second, electrons donated by activated adrenaline molecules are transferred via the surface of N-MCNT to activated oxygen molecules and turn them into ROS (mainly H_2O_2). Finally, the generated H_2O_2 oxidizes activated adrenaline to adrenochrome at the surface of N-MCNT.

Similar to oxygen molecules, N-MCNT exhibited much stronger adsorption affinity for adrenaline compared to MCNT. Under the same experimental settings, the single-point adsorption distribution coefficient (K_d) was 900 ± 200 L/kg (standard deviation calculated from three replicates) for N-MCNT, but only 380 ± 50 L/kg for MCNT. The two strong electron-donating phenolic groups in adrenaline make it an ideal π-electron-donor molecule. Accordingly, doping heteroatoms into the graphitic lattice of carbon nanomaterials markedly increases the polarizability of the graphitized carbons.[49] This implies that the $\pi-\pi$ electron−donor−acceptor (EDA) interaction between the adrenaline molecule (π-electron donor) and the highly polarized graphitic N-containing aromatic ring (π-electron acceptor) on N-MCNT would be favored when compared with that on MCNT.[50,51] The $\pi-\pi$ EDA mechanism is expected to facilitate electron transfer from the adrenaline molecule to the surface of N-MCNT, leading to the activation of adrenaline (electron donor/reductant). In addition to the two phenol groups, the secondary amine group [pK_a = 9.84 (Figure S1)] in adrenaline has strong basicity and may act as an efficient electron donor when adsorbed and deprotonated at the surface of N-MCNT. In line with this hypothesis, a previous study[52] reported that under dark conditions carboxylated single-walled carbon nanotubes could generate H_2O_2 and $O_2^{\bullet-}$ from molecular oxygen in water in the presence of biomoleucle NADH (β-nicotinamide adenine dinucleotide, reduced form) whose reducing capability is enabled by the heterocyclic amine group. This improves our understanding of the cytotoxicity of carbon nanomaterials.

Adrenaline activation by specific adsorption at the π-electron-acceptor sites on N-MCNT is a key step for the initiation of the whole reaction process. This is evidenced by the linear relationship (R^2 = 0.98) observed between the reciprocal of the initial oxidation rate of adrenaline ($1/r_0$) and

https://dx.doi.org/10.1021/acsestwater.0c00003
ACS EST Water 2021, 1, 79−88

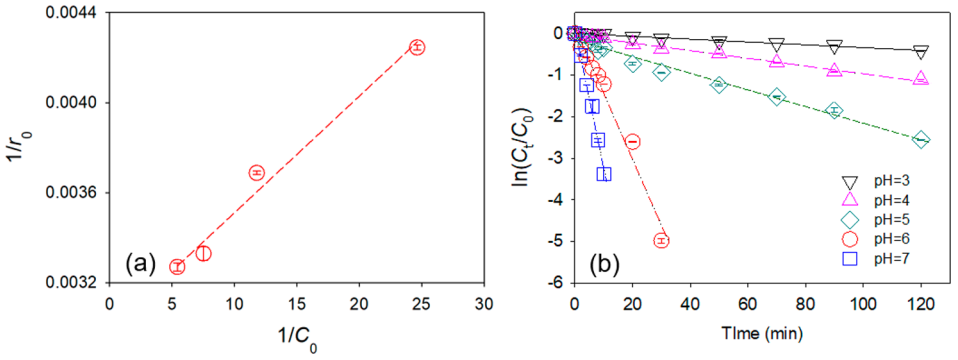

Figure 5. Degradation of adrenaline in the presence of N-MCNT (150 mg/L) under different conditions. (a) Relationship of the reciprocal of the initial oxidation rate ($1/r_0$) and the reciprocal of the initial adrenaline concentration ($1/C_0$) (0.04, 0.08, 0.13, and 0.18 mM) at pH 6 with phosphate buffer. (b) Pseudo-first-order degradation kinetics of adrenaline (initially at 0.18 mM) at different pHs buffered with phosphate plotted as $\ln(C_t/C_0)$ vs time. Error bars represent standard variations calculated from duplicate samples. Lines are for visual clarity only.

the reciprocal of the initial adrenaline concentration ($1/C_0$) (Figure 5a), which is commonly known as the Langmuir–Hinsheiwood model.[53,54] The adsorption-controlled activation mechanism can partially explain the strong pH dependence of adrenaline oxidation catalyzed by N-MCNT (Figure 5b). As the pH was increased from 3 to 7, the reaction was remarkably accelerated as reflected by a 95-fold increase in the calculated apparent pseudo-first-order rate constant (k_{obs}) from $(3.40 \pm 0.02) \times 10^{-3}$ to $(3.22 \pm 0.02) \times 10^{-1}$ min^{-1}. Accordingly, adsorption of adrenaline (initially at 0.18 mM) on N-MCNT (measured in the absence of oxygen) was considerably enhanced by increasing the pH from 3 to 7 (K_d increased from 1100 ± 300 to 8000 ± 3000 L/kg), which resulted from the facilitated $\pi-\pi$ EDA interaction.[51] Additionally, the enhanced adrenaline oxidation at higher pH is likely due to the higher molecular electron density as the electron-donating ability of the phenolic group in adrenaline improves when it is dissociated to the negatively charged form [pK_{as} = 8.63 and 13.13 (Figure S1)]. The contrasting oxidation rates observed among adrenaline, dopamine, and paracetamol could also stem from their very different electron-donor abilities. Unlike adrenaline and dopamine, paracetamol has only one phenolic group, and its amine group is conjugated with the carbonyl group, resulting in the weakest electron-donor ability. On the other hand, the higher basicity of the secondary amine group in adrenaline relative to the primary amine group in dopamine leads to stronger electron-donor ability and thus greater susceptibility to activation and oxidation at the surface of N-MCNT. Similarly, the kinetics of oxidation of phenols by carbon nanotube-activated peroxydisulfate was found to be positively correlated with the electron-donating ability of the substituted groups on the phenols.[55] Note these three ACPs (all initially at 0.06 mM) showed comparable adsorption affinities for N-MCNT under the same conditions; the K_d values were 23000 ± 1000, 30000 ± 3000, and 21500 ± 500 L/kg for adrenaline, dopamine, and paracetamol, respectively. In spite of the much poorer electron-donor ability, paracetamol exhibited an adsorption affinity close to those of adrenaline and dopamine, which could be reconciled by the greater contribution from the hydrophobic effect due to the less polar/ionic functional groups.

The transfer of electrons on the surface of N-MCNT from the adsorbed adrenaline molecules to the adsorbed oxygen molecules is essential to the activation of both species. The presence of conduction electrons at the surface of N-MCNT was verified by EPR spectra (Figure S11). Despite the low intensity, the EPR signal originated from conduction electrons[56] as characterized by a *g*-factor at approximately 1.9918 that was evident on N-MCNT in the presence of both adrenaline and dissolved oxygen, but not on MCNT given the same conditions or on N-MCNT in the absence of dissolved oxygen. Note the π-electron-acceptor sites (graphitic N-containing aromatic rings) on N-MCNT have a certain Lewis acidity; therefore, the adrenaline molecule and the oxygen molecule are activated by the Lewis acid site and Lewis base site on N-MCNT, respectively. Compared with MNCT, N-MCNT are expected to have a higher electron conductivity[57] that would facilitate the electron transfer process on the surface. However, the mechanism of enhanced electron transfer alone could not account for the activation of oxygen, and the following oxidation of adrenaline as pure graphite exhibited little catalytic activity in the reaction (Figure 1) despite the electron conductivity being much higher than that of carbon nanotubes.[58] Another point worth noting is that besides conduction electrons, protons are required for activation of oxygen molecules to generate ROS.[26] Although four protons are released when an adrenaline molecule is oxidized to adrenochrome, the protons needed in oxygen activation can be from only an aqueous solution, as the ROS (mainly H_2O_2) responsible for adrenaline oxidation cannot be generated without first activating oxygen to H_2O_2. This is why the oxidation of adrenaline was completely terminated by replacing the phosphate buffer solution with neat DMSO (a proton-free solvent) (Figure 2).

Implication. This study describes a novel light-independent process for oxidizing ACPs by aqueous dissolved oxygen via simultaneous activation of target organic compounds at the Lewis acid sites and oxygen molecules at the Lewis base sites on the surface of nitrogen-doped carbon nanomaterials. One great benefit of this approach is that the oxidation of ACPs is a unidirectional catalytic reaction that minimizes chemical addition (no oxidants) and energy requirements (no UV light). Notably, adrenaline is a useful biomarker for human physiological conditions and/or disorders, and an accurate detection and quantification technique is urgently needed. The existing adrenaline detection techniques often require the transformation of adrenaline to adrenochrome as a prerequisite for measurement, which is often implemented by relatively complex electrochemical oxidation methods.[59,60] We here offer an alternative and convenient way to completely oxidize

https://dx.doi.org/10.1021/acsestwater.0c00003
ACS EST Water 2021, 1, 79–88

adrenaline to adrenochrome as a sole product under mild conditions. Finally, although complete mineralization of the target ACPs was not achieved in this study, the ROS (mainly H_2O_2) generated from the self-sensitization of ACPs catalyzed by N-MCNT can be readily utilized to produce more oxidizing species (•OH) when coupled with Fenton-like reactions initiated by adding Fe(II) salts or induced by electro-activation. More research is warranted to explore this hypothesis.

■ ASSOCIATED CONTENT

Supporting Information

The Supporting Information is available free of charge at https://pubs.acs.org/doi/10.1021/acsestwater.0c00003.

Fitting kinetic parameters of oxidation reactions of the ACPs (Table S1), molecular structures and pK_{as} values of ACPs (Figure S1), schematic diagram of the CFCL system (Figure S2), HRTEM image and EDS elemental mapping of N-MCNT (Figure S3), comparison of water contact angles of N-MCNT and MCNT (Figure S4), mass spectroscopic analysis results of oxidation products of ACPs (Figures S5−S7), oxidation pathways of ACPs (Figures S8 and S9), EPR spectra of $O_2^{\bullet-}$ in the supernatant (Figure S10), and EPR spectra of N-MCNT and MCNT before and after reaction with adrenaline (Figure S11) (PDF)

■ AUTHOR INFORMATION

Corresponding Author

Dongqiang Zhu − *School of Urban and Environmental Sciences, Key Laboratory of the Ministry of Education for Earth Surface Processes, Peking University, Beijing 100871, China;* orcid.org/0000-0001-6190-5522; Phone: +86 (010) 62766405; Email: zhud@pku.edu.cn

Authors

Langsha Yi − *School of Urban and Environmental Sciences, Key Laboratory of the Ministry of Education for Earth Surface Processes, Peking University, Beijing 100871, China*

Chenhui Wei − *School of Urban and Environmental Sciences, Key Laboratory of the Ministry of Education for Earth Surface Processes, Peking University, Beijing 100871, China*

Wanchao Yu − *State Key Laboratory of Environmental Chemistry and Eco-toxicology, Research Center for Eco-environmental Sciences, Chinese Academy of Sciences, Beijing 100085, China*

Heyun Fu − *State Key Laboratory of Pollution Control and Resource Reuse, School of the Environment, Nanjing University, Jiangsu 210046, China;* orcid.org/0000-0002-0014-1829

Xiaolei Qu − *State Key Laboratory of Pollution Control and Resource Reuse, School of the Environment, Nanjing University, Jiangsu 210046, China;* orcid.org/0000-0002-9157-4274

Pedro J. J. Alvarez − *Department of Civil and Environmental Engineering, Rice University, Houston, Texas 77251, United States;* orcid.org/0000-0002-6725-7199

Complete contact information is available at: https://pubs.acs.org/10.1021/acsestwater.0c00003

Notes

The authors declare no competing financial interest.

■ ACKNOWLEDGMENTS

This work was supported by the National Natural Science Foundation of China (Grants 21920102002 and 41991331). Partial funding for P.J.A. was provided by the NSF ERC on Nanotechnology-Enabled Water Treatment (EEC-1449500).

■ REFERENCES

(1) Buser, H. R.; Poiger, T.; Müller, M. D. Occurrence and environmental behavior of the chiral pharmaceutical drug ibuprofen in surface waters and in wastewater. *Environ. Sci. Technol.* **1999**, *33*, 2529−2535.

(2) Rabiet, M.; Togola, A.; Brissaud, F.; Seidel, J. L.; Budzinski, H.; Elbaz-Poulichet, F. Consequences of treated water recycling as regards pharmaceuticals and drugs in surface and ground waters of a medium-sized mediterranean catchment. *Environ. Sci. Technol.* **2006**, *40*, 5282−5288.

(3) Roberts, J.; Kumar, A.; Du, J.; Hepplewhite, C.; Ellis, D. J.; Christy, A. G.; Beavis, S. G. Pharmaceuticals and personal care products (PPCPs) in Australia's largest inland sewage treatment plant, and its contribution to a major Australian river during high and low flow. *Sci. Total Environ.* **2016**, *541*, 1625−1637.

(4) Wu, M.; Xiang, J.; Que, C.; Chen, F.; Xu, G. Occurrence and fate of psychiatric pharmaceuticals in the urban water system of Shanghai, China. *Chemosphere* **2015**, *138*, 486−493.

(5) Loraine, G. A.; Pettigrove, M. E. Seasonal variations in concentrations of pharmaceuticals and personal care products in drinking water and reclaimed wastewater in southern California. *Environ. Sci. Technol.* **2006**, *40*, 687−695.

(6) Ternes, T. A.; Meisenheimer, M.; Mcdowell, D.; Sacher, F.; Brauch, H. J.; Haist-Gulde, B.; Preuss, G.; Wilme, U.; Zulei-Seibert, N. Removal of pharmaceuticals during drinking water treatment. *Environ. Sci. Technol.* **2002**, *36*, 3855−3863.

(7) Mashayekh-Salehi, A.; Moussavi, G.; Yaghmaeian, K. Preparation, characterization and catalytic activity of a novel mesoporous nanocrystalline MgO nanoparticle for ozonation of acetaminophen as an emerging water contaminant. *Chem. Eng. J.* **2017**, *310*, 157−169.

(8) Jacobs, I. G.; Finn, J. C.; Jelinek, G. A.; Oxer, H. F.; Thompson, P. L. Effect of adrenaline on survival in out-of-hospital cardiac arrest: A randomised double-blind placebo-controlled trial. *Resuscitation* **2011**, *82*, 1138−1143.

(9) Benotti, M. J.; Stanford, B. D.; Wert, E. C.; Snyder, S. A. Evaluation of a photocatalytic reactor membrane pilot system for the removal of pharmaceuticals and endocrine disrupting compounds from water. *Water Res.* **2009**, *43*, 1513−1522.

(10) Mompelat, S.; Le Bot, B.; Thomas, O. Occurrence and fate of pharmaceutical products and by-products, from resource to drinking water. *Environ. Int.* **2009**, *35*, 803−814.

(11) Roberts, P. H.; Thomas, K. V. The occurrence of selected pharmaceuticals in wastewater effluent and surface waters of the lower Tyne catchment. *Sci. Total Environ.* **2006**, *356*, 143−153.

(12) Ternes, T. A. Occurrence of drugs in German sewage treatment plants and rivers. *Water Res.* **1998**, *32*, 3245−3260.

(13) Imaeda, A. B.; Watanabe, A.; Sohail, M. A.; Mahmood, S.; Mohamadnejad, M.; Sutterwala, F. S.; Flavell, R. A.; Mehal, W. Z. Acetaminophen-induced hepatotoxicity in mice is dependent on Tlr9 and the Nalp3 inflammasome. *J. Clin. Invest.* **2009**, *119*, 305−314.

(14) Segura-Aguilar, J.; Paris, I.; Muñoz, P.; Ferrari, E.; Zecca, L.; Zucca, F. A. Protective and toxic roles of dopamine in Parkinson's disease. *J. Neurochem.* **2014**, *129*, 898−915.

(15) Tang, W.; Weil, M. H.; Sun, S.; Noc, M.; Yang, L.; Gazmuri, R. J. Epinephrine increases the severity of postresuscitation myocardial dysfunction. *Circulation* **1995**, *92*, 3089−3093.

(16) Antoni, M. H.; Lutgendorf, S. K.; Cole, S. W.; Dhabhar, F. S.; Sephton, S. E.; McDonald, P. G.; Stefanek, M.; Sood, A. K. The influence of bio-behavioural factors on tumour biology: Pathways and mechanisms. *Nat. Rev. Cancer* **2006**, *6*, 240−248.

(17) Feng, M.; Baum, J. C.; Nesnas, N.; Lee, Y.; Huang, C.-H.; Sharma, V. K. Oxidation of sulfonamide antibiotics of six-membered

heterocyclic moiety by Ferrate(VI): Kinetics and mechanistic insight into SO_2 extrusion. *Environ. Sci. Technol.* **2019**, *53*, 2695−2704.
(18) Anipsitakis, G. P.; Dionysiou, D. D. Degradation of organic contaminants in water with sulfate radicals generated by the conjunction of peroxymonosulfate with cobalt. *Environ. Sci. Technol.* **2003**, *37*, 4790−4797.
(19) Zhang, J.; Sun, B.; Xiong, X.; Gao, N.; Song, W.; Du, E.; Guan, X.; Zhou, G. Removal of emerging pollutants by Ru/TiO_2-catalyzed permanganate oxidation. *Water Res.* **2014**, *63*, 262−270.
(20) Xiao, R.; Ma, J.; Luo, Z.; Zeng, W.; Wei, Z.; Spinney, R.; Hu, W.; Dionysiou, D. D. Experimental and theoretical insight into hydroxyl and sulfate radicals-mediated degradation of carbamazepine. *Environ. Pollut.* **2020**, *257*, 113498.
(21) von Gunten, U. Ozonation of drinking water: Part II Disinfection and by-product formation in presence of bromide, iodide or chlorine. *Water Res.* **2003**, *37*, 1469−1487.
(22) Yang, Q.; Choi, H.; Al-Abed, S. R.; Dionysiou, D.D. Iron-cobalt mixed oxide nanocatalysts: Heterogeneous peroxymonosulfate activation, cobalt leaching, and ferromagnetic properties for environmental applications. *Appl. Catal., B* **2009**, *88*, 462−469.
(23) Qu, X.; Brame, J.; Li, Q.; Alvarez, P. J. J. Nanotechnology for a safe and sustainable water supply: Enabling integrated water treatment and reuse. *Acc. Chem. Res.* **2013**, *46*, 834−843.
(24) Liu, X.; Dai, L. Carbon-based metal-free catalysts. *Nat. Rev. Mater.* **2016**, *1*, 16064.
(25) Deng, D.; Novoselov, K. S.; Fu, Q.; Zheng, N.; Tian, Z.; Bao, X. Catalysis with two-dimensional materials and their heterostructures. *Nat. Nanotechnol.* **2016**, *11*, 218−230.
(26) Guo, D.; Shibuya, R.; Akiba, C.; Saji, S.; Kondo, T.; Nakamura, J. Active sites of nitrogen-doped carbon materials for oxygen reduction reaction clarified using model catalysts. *Science* **2016**, *351*, 361−365.
(27) Gong, K.; Du, F.; Xia, Z.; Durstock, M.; Dai, L. Nitrogen-doped carbon nanotube arrays with high electrocatalytic activity for oxygen reduction. *Science* **2009**, *323*, 760−764.
(28) Haider, M. R.; Jiang, W.; Han, J.; Sharif, H. M. A.; Ding, Y.; Cheng, H.; Wang, A. In-situ electrode fabrication from polyaniline derived N-doped carbon nanofibers for metal-free electro-Fenton degradation of organic contaminants. *Appl. Catal., B* **2019**, *256*, 117774.
(29) Sun, H.; Kwan, C. K.; Suvorova, A.; Ang, H. M.; Tadé, M. O.; Wang, S. Catalytic oxidation of organic pollutants on pristine and surface nitrogen-modified carbon nanotubes with sulfate radicals. *Appl. Catal., B* **2014**, *154*−*155*, 134−141.
(30) Guan, C.; Jiang, J.; Pang, S.; Luo, C.; Ma, J.; Zhou, Y.; Yang, Y. Oxidation kinetics of bromophenols by nonradical activation of peroxydisulfate in the presence of carbon nanotube and formation of brominated polymeric products. *Environ. Sci. Technol.* **2017**, *51*, 10718−10728.
(31) Chen, H.; Yang, Y.; Hu, Z.; Huo, K.; Ma, Y.; Chen, Y.; Wang, X.; Lu, Y. Synergism of C_5N six-membered ring and vapor-liquid-solid growth of CN_x nanotubes with pyridine precursor. *J. Phys. Chem. B* **2006**, *110*, 16422−16427.
(32) Lu, C. Y.; Chiu, H. S. Adsorption of zinc (II) from water with purified carbon nanotubes. *Chem. Eng. Sci.* **2006**, *61*, 1138−1145.
(33) Marques, F.; Duarte, R. O.; Moura, J. J. G.; Bicho, M. P. Conversion of adrenaline to indolic derivatives by the human erythrocyte plasma membrane. *Neurosignals* **2004**, *5*, 275−282.
(34) Suda, I.; Takahashi, H. Degradation of methyl and ethyl mercury into inorganic mercury by other reactive oxygen species. *Arch. Toxicol.* **1992**, *66*, 34−39.
(35) Tai, C.; Li, Y.; Yin, Y. G.; Scinto, L. J.; Jiang, G.; Cai, Y. Methylmercury photodegradation in surface water of the Florida Everglades: Importance of dissolved organic matter-methylmercury complexation. *Environ. Sci. Technol.* **2014**, *48*, 7333−7340.
(36) Halladja, S.; ter Halle, A.; Aguer, J.-P.; Boulkamh, A.; Richard, C. Inhibition of humic substances mediated photooxygenation of furfuryl alcohol by 2,4,6-trimethylphenol: Evidence for reactivity of the phenol with humic triplet excited states. *Environ. Sci. Technol.* **2007**, *41*, 6066−6073.
(37) Yuan, H.; Pan, H.; Shi, J.; Li, H.; Dong, W. Kinetics and mechanisms of reactions for hydrated electron with chlorinated benzenes in aqueous solution. *Front. Environ. Sci. Eng.* **2015**, *9*, 583−590.
(38) Wilkinson, F.; Helman, W. P.; Ross, A. B. Rate constants for the decay and reactions of the lowest electronically excited singlet state of molecular oxygen in solution. an expanded and revised compilation. *J. Phys. Chem. Ref. Data* **1995**, *24*, 663−677.
(39) Dong, F.; Li, Q.; Sun, Y.; Ho, W.-K. Noble metal-like behavior of plasmonic Bi particles as a cocatalyst deposited on $(BiO)_2CO_3$, microspheres for efficient visible light photocatalysis. *ACS Catal.* **2014**, *4*, 4341−4350.
(40) Alia; Mohanty, P.; Matysik, J. Effect of proline on the production of singlet oxygen. *Amino Acids* **2001**, *21*, 195−200.
(41) Wang, D.; Zhao, L.; Guo, L.; Zhang, H. Online detection of reactive oxygen species in ultraviolet (UV)-irradiated nano-TiO_2 suspensions by continuous flow chemiluminescence. *Anal. Chem.* **2014**, *86*, 10535−10539.
(42) Mcdowell, D. C.; Huber, M. M.; Wagner, M.; von Gunten, U.; Ternes, T.A. Ozonation of Carbamazepine in Drinking Water: Identification and kinetic study of major oxidation products. *Environ. Sci. Technol.* **2005**, *39*, 8014−8022.
(43) Klavarioti, M.; Mantzavinos, D.; Kassinos, D. Removal of residual pharmaceuticals from aqueous systems by advanced oxidation processes. *Environ. Int.* **2009**, *35*, 402−417.
(44) Khetan, S. K.; Collins, T. J. Human pharmaceuticals in the aquatic environment: A challenge to green chemistry. *Chem. Rev.* **2007**, *107*, 2319−2364.
(45) Mantzavinos, D.; Psillakis, E. Enhancement of biodegradability of industrial wastewaters by chemical oxidation pre-treatment. *J. Chem. Technol. Biotechnol.* **2004**, *79*, 431−454.
(46) Chamapro, E.; Marco, A.; Esplugas, E. Use of Fenton reagent to improve organic chemical biodegradability. *Water Res.* **2001**, *35*, 1047−1051.
(47) Santos, L.; Tipping, P. G. Attenuation of adjuvant arthritis in rats by treatment with oxygen radical scavengers. *Immunol. Cell Biol.* **1994**, *72*, 406−414.
(48) Cojocariu, A. M.; Mutin, P. H.; Dumitriu, E.; Vioux, A.; Fajula, F.; Hulea, V. Removal of dimethylsulfoxide from wastewater using mild oxidation with H_2O_2 over Ti-based catalysts. *Chemosphere* **2009**, *77*, 1065−1068.
(49) Ranjbar Sahraie, N.; Paraknowitsch, J. P.; Göbel, C.; Thomas, A.; Strasser, P. Noble-metal-free electrocatalysts with enhanced ORR performance by task-specific functionalization of carbon using ionic liquid precursor systems. *J. Am. Chem. Soc.* **2014**, *136*, 14486−14497.
(50) Yi, L.; Zuo, L.; Wei, C.; Fu, H.; Qu, X.; Zheng, S.; Xu, Z.; Guo, Y.; Li, H.; Zhu, D. Enhanced adsorption of bisphenol A, tylosin, and tetracycline from aqueous solution to nitrogen-doped multiwall carbon nanotubes. *Sci. Total Environ.* **2020**, *719*, 137389.
(51) Zuo, L.; Guo, Y.; Li, X.; Fu, H.; Qu, X.; Zheng, S.; Gu, C.; Zhu, D.; Alvarez, P. J. J. Enhanced adsorption of hydroxyl- and amino-substituted aromatic chemicals to nitrogen-doped multiwall carbon nanotubes: A combined batch and theoretical calculation study. *Environ. Sci. Technol.* **2016**, *50*, 899−905.
(52) Hsieh, H.-S.; Wu, R.; Jafvert, C. T. Light-Independent reactive oxygen species (ROS) formation through electron transfer from carboxylated single-walled carbon nanotubes in water. *Environ. Sci. Technol.* **2014**, *48*, 11330−11336.
(53) Pintar, A.; Batista, J.; Levec, J.; Kajiuchi, T. Kinetics of the catalytic liquid-phase hydrogenation of aqueous nitrate solutions. *Appl. Catal., B* **1996**, *11*, 81−98.
(54) De Pedro, Z. M.; Casas, J. A.; Gomez-Sainero, L. M.; Rodriguez, J. J. Hydrodechlorination of dichloromethane with a Pd/AC catalyst: Reaction pathway and kinetics. *Appl. Catal., B* **2010**, *98*, 79−85.
(55) Ren, W.; Xiong, L.; Yuan, X.; Yu, Z.; Zhang, H.; Duan, X.; Wang, S. Activation of peroxydisulfate on carbon nanotubes:

https://dx.doi.org/10.1021/acsestwater.0c00003
ACS EST Water 2021, 1, 79−88

Electron-transfer mechanism. *Environ. Sci. Technol.* **2019**, *53*, 14595−14603.
(56) Bandow, S.; Asaka, S.; Zhao, X.; Ando, Y. Purification and magnetic properties of carbon nanotubes. *Appl. Phys. A: Mater. Sci. Process.* **1998**, *A67*, 23−27.
(57) Wiggins-Camacho, J. D.; Stevenson, K. J. Effect of nitrogen concentration on capacitance, density of states, electronic conductivity, and morphology of N-doped carbon nanotube electrodes. *J. Phys. Chem. C* **2009**, *113*, 19082−19090.
(58) Marinho, B.; Ghislandi, M.; Tkalya, E.; Koning, C. E.; de With, G. Electrical conductivity of compacts of graphene, multi-wall carbon nanotubes, carbon black, and graphite powder. *Powder Technol.* **2012**, *221*, 351−358.
(59) Nikolajsen, R. P. H.; Hansen, Å. M. Analytical methods for determining urinary catecholamines in healthy subjects. *Anal. Chim. Acta* **2001**, *449*, 1−15.
(60) Ribeiro, J. A.; Fernandes, P. M. V.; Pereira, C. M.; Silva, F. Electrochemical sensors and biosensors for determination of catecholamine neurotransmitters: A review. *Talanta* **2016**, *160*, 653−679.

https://dx.doi.org/10.1021/acsestwater.0c00003
ACS EST Water 2021, 1, 79−88